Pattern and structure of microtopography implies autogenic origins in forested wetlands

Jacob S. Diamond[1,2], Daniel L. McLaughlin[3], Robert A. Slesak[4], and Atticus Stovall[5]

[1]Quantitative Ecohydrology Laboratory, RiverLy, Irstea, Lyon, 69100, France
[2]Continental Hydrogeosytems Laboratory, University of Tours, Tours 37200, France
[3]School of Forest Resources and Environmental Conservation, Virginia Tech, Blacksburg, 24060, USA
[4]Minnesota Forest Resources Council, St. Paul, 55108, USA
[5]NASA Goddard Space Flight Center, Greenbelt, 20771, USA

Correspondence to: Jacob S. Diamond (jacdia@vt.edu)

Abstract

Wetland microtopography is a visually striking feature, but also critically influences biogeochemical processes at both the scale of its observation (10^{-2}–10^2 m^2) and at aggregate scales (10^2–10^4 m^2). However, relatively little is known about how wetland microtopography develops or the factors influencing its structure and pattern. Growing research across different ecosystems suggests that reinforcing processes may be common between plants and their environment, resulting in self-organized patch features, like hummocks. Here, we used landscape ecology metrics and diagnostics to evaluate the plausibility of plant-environment feedback mechanisms in the maintenance of wetland microtopography. We used terrestrial laser scanning (TLS) to quantify the sizing and spatial distribution of hummocks in 10 black ash (*Fraxinus nigra* Marshall) wetlands in northern Minnesota, U.S.A. We observed clear elevation bimodality in our wettest sites, indicating microsite divergence into two states: elevated hummocks and low elevation hollows. We coupled the TLS dataset to a three-year water level record and soil-depth measurements, and showed that hummock height (mean = 0.31±0.06 m) variability is largely predicted by mean water level depth (R^2=0.8 at the site scale, R^2=0.12–0.56 at the hummock scale), with little influence of subsurface microtopography on surface microtopography. Hummocks in wetter sites exhibited regular spatial patterning (i.e., regular spacing of ca. 1.5 meters, 25–30% further apart than expected by chance) in contrast to the more random spatial arrangements of hummocks in drier sites. Hummock size distributions (perimeters, areas, and volumes) were lognormal, with a characteristic patch area of approximately 1 m^2 across sites. Hummocks increase the effective soil surface area for redox gradients and exchange interfaces in black ash wetlands by up to 32%, and influence surface water dynamics through modulation of specific yield by up to 30%. Taken together, the data support the hypothesis that vegetation develops and maintains hummocks in response to anaerobic stresses from saturated soils, with a potential for a microtopographic signature of life.

Key words: hummocks, hollows, black ash, Fraxinus nigra, wetlands, ecohydrology, TLS

1   Introduction

Microtopography, or the small-scale structured variation (10^{-1}–10^0 m) in ground surface height, is common to many ecosystems. Wetland microtopography is particularly well studied, and is found in freshwater marshes (Van de Koppel et al., 2006), fens (Sullivan et al., 2008), peat bogs (Nungesser, 2003), forested swamps (Bledsoe and Shear, 2000), tidal freshwater swamps (Duberstein et al., 2013), and coastal marshes (Stribling et al., 2007). Wetland

microtopography is common enough that researchers in disparate systems collectively refer to local high points as "hummocks" and local low points as "hollows". Hollows are more frequently inundated and typically comprise large, flat or concave open spaces, whereas elevated hummocks tend to be dispersed throughout hollows (Nungesser, 2003; Stribling et al., 2007). Elevated hummocks, even centimeters taller than adjacent hollows, can provide enough soil aeration to limit anaerobic stress to vegetation, promoting higher plant abundance and primary production (Strack et al., 2006; Rodríguez-Iturbe et al., 2007; Sullivan et al., 2008).

Wetland microtopography changes the spatial distribution of relative water levels, affecting vegetative composition and growth, which, in turn, may reinforce microtopographic development. For example, seedlings often fare better on elevated microtopographic features such as downed woody debris or tree-fall mounds (Huenneke & Sharitz, 1990). The resulting increased vegetation root growth and associated organic matter inputs on such features may subsequently support hummock expansion. In this way, vegetation may reinforce and maintain its own hummock microtopography (and thus preferred environmental conditions). Growing research across different ecosystems suggests that such reinforcing processes, or feedback loops, may be common between biota and their environment, and may result in characteristic, self-organized patch features (Rietkerk and van de Koppel, 2008; Bertolini et al., 2019). By quantifying the structure and patterning of these features, we may therefore make process-based inferences about latent feedback mechanisms (Turner, 2005; Quintero and Cohen 2019).

Spatial patterning of landscape patches has been observed in many systems, such as the striping of vegetated patches in arid settings or maze-like patterns in mussel beds (Rietkerk and van de Koppel, 2008), where researchers have inferred responsible feedback mechanisms (as opposed to random processes) using a suite of diagnostic indicators. There is a large body of literature where such measurements are used to identify patterned systems and to infer their latent feedbacks (see Pascual et al., 2002; Pascual and Guichard, 2005; Kefi et al., 2011; Kéfi et al., 2014; Quinton and Cohen, 2019 and references therein). We suggest that these diagnostic indicators are extensible to analysis of wetland microtopography, thereby allowing us to assess mechanisms that maintain and reinforce patterns of hummock patches. Here, we focus on three common methods of inference. First, multimodal distributions in environmental variables, such as vegetation composition, soil texture, and, in our case, elevation (and see Rietkerk et al., 2004; Eppinga et al., 2008; Watts et al., 2010), indicate positive feedbacks to patch growth, where local patch conditions promote further patch expansion (Scheffer and Carpenter, 2003; Pugnaire et al., 1996). Second, presence of characteristic patch sizes implies that limits to patch growth operate at local scales as opposed to system scales (Manor

65 and Shnerb, 2008; von Hardenberg et al., 2010). Limited patch growth results in a distinct absence of large patches, and a thus a truncation of the size distribution (Kéfi et al., 2014; Watts et al., 2014). Third, regular spatial patterning of patches (Rietkerk et al., 2004), or spatial overdispersion of patches (i.e., uniformity of patch spacing is greater than expected by chance), implies a coupling of both local-scale positive feedbacks to patch growth and local-scale negative feedbacks to patch expansion (Watts et al., 2014; Quinton and Cohen, 2019). Here, we extend this inferential

70 theoretical framework to characterize patterning and infer genesis and persistence of wetland microtopography.

Our conceptual model of wetland microtopographic development posits elevation-plant productivity feedbacks that result in elevation bimodality, characteristic patch sizes, and patch overdispersion (Figure 1). We suggest that many mechanisms may initiate microtopographic development, including direct actions from biota (e.g., burrowing or mounding), indirect actions from biota (e.g., tree falls or preferential litter accumulation), and abiotic events that

75 redistribute soils and sediment (e.g., extreme weather events). However, regardless of initiation mechanism, we hypothesize that elevated microsites provide relief from hydrologically induced anaerobic conditions, promoting plant establishment and growth, evapoconcentration of nutrients (Eppinga et al., 2009), increased organic matter accumulation and subsequent soil elevation (Harris et al. 2019), and so on (top, solid loop in Figure 1). These positive feedbacks ultimately induce soil elevation bimodality, where microtopographic features belong either to a stable

80 hummock and stable hollow elevation state (Rietkerk et al., 2004, Eppinga et al., 2008, Watts et al., 2010). Negative feedbacks eventually limit this growth; otherwise, hummocks would have no vertical or lateral limit. Vertical negative feedbacks may result from increased decomposition as hummocks grow vertically and their soils become more aerobic (Minick et al., 2019a; Minick et al., 2019b; bottom, dashed loop in Figure 1). Lateral negative feedbacks may result from canopy competition for light among trees located on hummocks, or from competition for nutrients among

85 hummocks (Rietkerk et al., 2004; Schroder et al., 2005; Eppinga et al., 2009), leading to spatial overdispersion and common patch sizes. Finally, we predict that the strength of these feedback loops that grow and maintain hummocks likely increase with wetter conditions (blue shading in Figure 1). In contrast, hummock-hollow terrain and pattern may be less evident in drier sites where soils are nearly always unsaturated and aerobic, weakening the elevation-productivity feedback (Miao et al., 2013; Miao et al., 2017). In a companion study we found support for this overall

90 model, where we observed vegetation and soil chemistry associations with hummock structures, indicative of elevation-productivity feedbacks, and that these associations were greatest in the wettest sites (Diamond et al., 2019).

Here, we add to that work by assessing the structure and pattern of hummock features and the extent to which they are influenced by hydrologic regime.

In this study, we evaluated wetland soil elevations, hummock spacing, and hummock sizes and their associations with hydrologic regimes in black ash (*Fraxinus nigra* Marshall) forested wetlands in northern Minnesota, U.S.A. To do so, we characterized microtopography with a 1-cm spatial resolution dataset from a terrestrial laser scanning (TLS) campaign. We also evaluated subsurface mineral layer topography and daily water levels to determine the extent that that these variables influenced observed surface microtopography. Specifically, we tested the following predictions:

1. Elevation will exhibit a bimodal distribution, but the degree of bimodality and the overall variability in elevation will be greater in wetter sites than drier sites.

2. Surface topography will not reflect subsurface mineral topography, but will instead be representative of self-organizing processes at the soil surface.

3. Hummock heights will be positively correlated with water levels at site and within-site scales.

4. Hummock patches will exhibit spatial overdispersion, which will be more evident at wetter sites.

5. Cumulative distributions of hummock areas (and perimeters and volumes) will correspond to a family of truncated distributions (e.g., exponential or lognormal), indicating a characteristic patch size, with wetter sites exhibiting more large area hummocks than drier sites.

2   Methods

2.1   Site descriptions

To test our hypotheses, we investigated ten black ash wetlands of varying size and hydrogeomorphic landscape position in northern Minnesota, U.S.A. (Figure 2; Table 1). Thousands of meters of sedimentary rocks overlay an Archean granite bedrock geology in this region. Study sites are located on a glacial moraine landscape (400–430 m ASL) that is flat to gently rolling, with the black ash wetlands found in lower landscape positions that commonly grade into aspen or pine-dominated upland forests. The climate is continental, with mean annual precipitation of 700 mm and a mean growing season (May–October) temperature of 14.3°C (mean annual temperature = -1.1°C – 4.8°C; WRCC 2019). Annual precipitation is approximately two-thirds rain and one-third snowfall. Potential evapotranspiration (PET) is approximately 600–650 mm per year (Sebestyen et al., 2011). Detailed site histories were unavailable for the ten study wetlands, but silvicultural practices in black ash wetlands have been historically limited

in extent (D'Amato et al., 2018). Based on the available information (e.g., Erdmann et al., 1987; Kurmis and Kim, 1989), we surmise that our sites are late successional or climax communities and have not been harvested for at least a century.

As part of a larger effort to understand and characterize black ash wetlands (D'Amato et al., 2018), we categorized and grouped each wetland by its hydrogeomorphic characteristics as follows: 1) depression sites ("D", n = 4) characterized by a convex, pool-type geometry with geographical isolation from other surface water bodies and surrounded by uplands, 2) lowland sites ("L", n = 3) characterized by extensive wetland complexes on flat, gently sloping topography, and 3) transition sites ("T", n = 3) characterized as flat, linear boundaries between uplands and black spruce (*Picea mariana* Mill. Britton) bogs (Figure 3). The three lowland sites were control plots from a long-term experimental randomized block design on black ash wetlands (blocks 1, 3, and 6; Slesak et al., 2014; Diamond et al., 2018). We considered hydrogeomorphic variability among sites an important criterion, as it allowed us to capture expected differences in hydrologic regime and thus differences in the strength of our predicted control on microtopographic generation (Figure 1). Ground slopes across sites ranged from 0–1%. Black ash wetlands are typically hydrologically disconnected from regional groundwater and other surface water bodies, resulting in precipitation and evapotranspiration (ET) as dominant components of the water budget, with no indication of extreme surface flows (Slesak et al., 2014). Water levels follow a common annual trajectory of late-spring/early-summer inundation (10–50 cm) followed by ET-induced summer drawdown and belowground water levels (Slesak et al., 2014; Diamond et al., 2018). However, the degree of drawdown depends on local hydrogeomorphic setting; we observed considerably wetter conditions at depression and transition sites than at lowland sites.

2.1.1 Vegetation

Overstory vegetation at the ten sites is dominated by black ash, with tree densities ranging from 650 stems ha^{-1} (basal area = 195 m^2 ha^{-1}) at the driest lowland site to 1600 stems ha^{-1} (basal area = 40 m^2 ha^{-1}) at a much wetter depression site (across-site mean = 942 stems ha^{-1}; Diamond et al. 2019). At the lowland sites, other overstory species were negligible, but at the depression and transition sites there were minor cohorts of northern white-cedar (*Thuja occidentalis* L.), green ash (*Fraxinus pennsylvanica* Marshall), red maple (*Acer rubrum* L.), yellow birch (*Betula alleghaniensis* Britt.), balsam poplar (*Populus balsamifera* L.), and black spruce (*Picea mariana* Mill. Britton). Except at one transition site (T1), where northern white cedar represented a significant overstory component, black ash represented over 75% of overstory cover across all sites. Black ash also made up the dominant midstory component

in each site, but was regularly found with balsam fir (*Abies balsamea* L. Mill.) and speckled alder (*Alnus incana* L. Moench) in minor components, and greater abundances of American elm (*Ulmus Americana* L.) at lowland sites. Black ash stands are commonly highly uneven-aged (Erdmann et al., 1987), with canopy tree ages ranging from 130–

150   232 years, and stand development under a gap-scale disturbance regime (D'Amato et al., 2018). Black ash are also typically slow-growing, achieving heights of only 10–15 m and diameters at breast height of only 25–30 cm after 100 years (Erdmann et al., 1987). The relatively open canopies of black ash wetlands (leaf area index < 2.5; Telander et al., 2015) allow for a variety of graminoids, shrubs, and mosses to grow in the understory. However, the majority of understory diversity and biomass tends to occur on hummocks that are occupied by black ash trees (Diamond et al.,

155   2019). Hollows exhibit relatively little plant cover and are typically bare soil areas, but may be covered at times of the year by sedges (*Carex spp*.) or layers of duckweed (*Lemna minor* L.), especially after recent inundation.

2.1.2   Soils

Soils in black ash wetlands in this region tend to be Histosols characterized by deep mucky peats underlain by silty clay mineral horizons, although there were clear differences among site groups (NRCS 2019). Depression sites were

160   commonly associated with Terric haplosaprists of the poorly drained Cathro or Rifle series with O horizons approximately 30–150 cm deep (Table 1). Lowland sites were associated with lowland Histic inceptisols of the Wildwood series, which consist of deep, poorly drained mineral soils with a thin O horizon (< 10 cm) underlain by clayey till or glacial lacustrine sediments. Transition sites typically had the deepest O horizons (> 100 cm), and were associated with typic haplosaprists of the Seelyeville series and Typic haplohemists (NRCS 2019). Both depression

165   and transition sites had much deeper O horizons than lowland sites, but depression site organic soils were typically muckier and more decomposed than more peat-like transition site soils.

2.2   TLS

2.2.1   Data collection

To characterize the microtopography of our sites, we conducted a terrestrial laser scanning (TLS) campaign from

170   October 20–24, 2017. We chose this period to ensure high-quality TLS acquisitions, as it coincided with the time of least vegetative cover and the least likelihood for inundated conditions. During scanning, leaves from all deciduous canopy trees had fallen and grasses had largely senesced. Standing water was present at portions of three of the sites and was typically dispersed across the site in small pools (*ca*. 0.5–2 m^2) less than 10 cm deep. We used a Faro Focus

120 3D phase-shift TLS (905 nm λ) to scan three randomly established, 10 m diameter sampling plots at each site (see

175   Stovall et al., 2019 for exact methodological details). For each site, we merged our plot-level TLS data to a single

~900 m² site-level point-cloud using 30 strategically placed and scanned 7.62 cm radius polystyrene registration

spheres set atop 1.2 m stakes. We referenced each site to a datum located at each site's base well elevation (see section

2.3.1).

To validate the TLS surface model products, we installed sixty 2.54 cm radius spheres on fiberglass stakes exactly 1.2

180   m above ground surface at each site. With the validation locations we could easily calculate the exact surface elevation

(i.e., 1.2 m below a scanned sphere) of 60 points in space. We installed 39 (13 at each plot) validation spheres at points

according to a random walk sampling design, and placed 21 (7 at each plot) validation spheres on distinctive

hummock-hollow transitions. We placed the 1.2 m tall validation spheres approximately plumb to reduce errors due

to horizontal misalignment.

185   We processed the point clouds generated from the TLS sampling campaign to generate two products: 1) site-level 1-

cm resolution ground surface models, and 2) site-level delineations of hummocks and hollows. The details and

validation of this method are described completely in Stovall et al. (2019), but a brief summary is provided here.

2.2.2   Surface model processing and validation

For each site, we first filtered the site-level point-clouds in the CloudCompare software (Othmani et al., 2011) and

190   created an initial surface model with the absolute minima in a moving 0.5 cm grid. We removed tree trunks from this

initial surface model using a slope analysis and implemented a final outlier removal filter to ensure all points above

ground level were excluded. Our final site-level surface models meshed the remaining slope-filtered point cloud using

a local minima approach at 1 cm resolution. We validated this final 1-cm surface model using the 60 validation spheres

per site.

195   Before we analyzed surface models from each site, we first detrended sites that exhibited site-scale elevation gradients

(e.g., 0.02 cm m^{-1}). These gradients may obscure analysis of site-level relative elevation distributions (Planchon et al.,

2002), and our hypothesis relates to relative elevations of hummocks and hollows and not their absolute elevations.

We chose the best-detrended surface model based on adjusted R^2 values and observation of resultant residuals and

elevation distributions from three options: no detrend, linear detrend, and quadratic detrend. Five sites were detrended:

200   L2 was detrended with a linear model, and D1, D2, D4, and T1 were detrended with quadratic models. We then

subsampled each surface model to 10,000 points to speed up processing time as original surface models were

approximately 100,000,000 points. We observed no significant difference in results from the original surface model based on our subsampling routine.

2.2.3   Hummock delineation and validation

205   We classified the final surface model into two elevation categories: hummocks and hollows. We first classified hollows using a combination of normalized elevation and slope thresholds; hollows have less than average elevation and less than average slope. This combined elevation and slope approach avoided confounding hollows with the tops of hummocks since the tops of hummocks are typically flat or shallow sloped. We removed hollows and used the remaining area as our domain of potential hummocks.

210   Within the potential hummock domain, we segmented hummocks into individual features using a novel approach – TopoSeg (Stovall et al., 2019) – and thereby created a hummock-level surface model for each site. We first used the local maximum (Roussel and Auty, 2018) of a moving window to identify potential microtopographic structures for segmentation. The local maximum served as the "seed point" from which we then applied a modified watershed delineation approach (Pau et al., 2010). The watershed delineation inverts convex topographic features and finds the

215   edge of the "watershed", which in our case are hummock edges. The defined boundary was used to clip and segment hummock features into individual hummock surface models.

For each delineated hummock within all sites, we calculated perimeter length, total area, volume, and height distributions relative both to local hollow datum and to a site level datum. To calculate area, we summed total number of points in each hummock raster multiplied by the model resolution (1 cm^2). We calculated volume using the same

220   method as area, but multiplied by each points' height above the hollow surface. Perimeter was conservatively estimated by converting our raster-based hummock features into polygons and extracting the edge length from each hummock. We estimated lateral hummock area by modelling each hummock as a simple cone, and calculating the lateral surface area from previously estimated volume and height. We believe this conical estimation method to be a conservative representation of the average height around the perimeter of the hummock because real hummock shapes

225   are more undulating and complex than simple cones. We elected not to use a cylindrical model because we observed some tapering of hummocks from their base to their top. We note that a cylindrical model would increase lateral surface area estimation by approximately 15% compared to the conical model and therefore may provide an upper bound on our conservative estimates.

To validate the hummock delineation, we compared manually delineated and automatically delineated hummock size distributions at one depression site (D2) and one transition site (T1), both with clearly defined hummock features. We omitted using a lowland site for validation because none of these sites had obvious hummock features that we could manually delineate with confidence. We manually delineated hummocks for the D2 and T1 sites with a qualitative visual analysis of raw TLS scans using the clipping tool in CloudCompare (2018). Stovall et al. (2019) found no significant differences between the manual and automatically segmented hummock distributions, and feature geometry had an RMSE of less than ~20%.

After the automatic delineation procedure and subsequent validation, we performed a data cleaning procedure by manually inspecting outputs in the CloudCompare software. We eliminated clear hummock mischaracterization that was especially prevalent at the edges of sites, where point densities were low. We also excluded downed woody debris from further hummock analysis because, although these features may serve as nucleation points for future hummocks, they are not traditionally considered hummocks and their distribution does not relate to our broad hypotheses. Finally, we excluded delineated hummocks that were less than $0.1 \ m^2$ in area because we did not observe hummocks less than this size during our field visits. This delineation and manual cleaning process yielded point clouds of hummocks and hollows for every site that could be further analyzed.

2.2.4   Surface model performance

Validation of surface models using the validation spheres indicated that surface models were precise (RMSE = 3.67 $\pm$ 1 cm) and accurate (bias = 1.26 $\pm$ 0.1 cm) across all sites (Stovall et al. 2019). The gently sloping lowland sites (L) had substantially higher RMSE and bias than the transition (T) and depression (D) sites. The relatively high error of lowland site validation points resulted from either low point density or a complete absence of LiDAR returns. We observed overestimation of the surface model when TLS scans were unable to reach the ground surface, leading to the greatest overestimations in sites with dense grass cover (lowland sites). Overestimation was also common in locations with no LiDAR returns, such as small hollows, where the scanner's oblique view angle was unable to reach. Nonetheless, examination of the surface models indicated clear ability of the TLS to capture surface microtopography (Figure S1).

2.2.5 Hummock delineation performance

Hummocks delineated from our algorithm were generally consistent in distribution and dimension with manually delineated hummocks. However, the automatic delineation located hundreds of small (<0.1 m^2) "hummock" features that were not captured with manual delineation, which we attribute to our detrending procedure. We did not consider automatically delineated hummocks less than 0.1 m^2 in further analyses, as we did not observe hummocks smaller than this in the field. Both area and volume size distributions from the manual and automatic delineations were statistically indistinguishable for both t-test (p-value = 0.84 and 0.51, respectively) and Kolmogorov-Smirnov test (p-value = 0.40 and 0.88, respectively). Automatically delineated hummock area, perimeter:area, and volume estimates had 23%, 19.6%, and 24.1% RMSE, respectively, and the estimates were either unbiased or slightly negatively biased (-9.8 %, 0.2 %, and -11.9 %, respectively). We consider these errors to be well within the range of plausibility, especially considering the uncertainty involved in manual delineation of hummocks, both in the field and on the computer. Final delineations showed clear visual differences among site types in the spatial distributions of hummocks (Figure S2).

2.3 Field data collection

2.3.1 Hydrology

To address our hypothesis that hydrology is a controlling variable of microtopographic expression in black ash wetlands, we instrumented all 10 sites to continuously monitor water level dynamics and precipitation. Three sites (L1, L2, and L3; Slesak et al., 2014) were instrumented in 2011 and seven in June 2016 following the same protocols. At each site, we placed a fully-slotted observation well (schedule 40 PVC, 2-inch diameter, 0.010-inch-wide slots) at approximately the lowest elevation; at the flatter L sites, wells were placed at the approximate geographic center of each site. Ground surface at the well served as each site's datum (i.e., elevation = 0 m). We instrumented each well with a high-resolution total pressure transducer (HOBO U20L-04, resolution = 0.14 cm, average error = 0.4 cm) to record water level time series at 15-minute intervals. We dug each well with a hand auger to a depth associated with the local clay mineral layer and did not penetrate the mineral layer, which ranged from 30 cm below the soil surface to depths greater than 200 cm. We then backfilled each well with a clean, fine sand (20-40 grade). At each site, we also placed a dry well with the same pressure transducer model to measure temperature-buffered barometric pressure and frequency for barometric pressure compensation (McLaughlin and Cohen, 2011).

2.3.2   Mineral layer depth measurements

To quantify the control that underlying mineral layer microtopography has on surface microtopography, we conducted synoptic measurements of mineral layer depth and thus organic soil thickness at each site. Within each of the 10 m diameter plots used for TLS at each site, we took 13 measurements (co-located with the randomly established validation spheres) of depth to mineral layer using a steel 1.2 m rod. At each point the steel rod was gently pushed into the soil with consistent pressure until resistance was met and the depth to resistance was recorded (resolution = 1 cm) as the depth to mineral layer. We then associated each of these depth-to-mineral-layer measurements with a soil elevation based on TLS data and the site-level datum (i.e., elevation at the base of each site's well).

2.4   Data analysis

2.4.1   Hydrology

We calculated simple hydrologic metrics based on the three years (2016–2018) of water level data for each site. For each site, we calculated the mean and variance of water level elevation relative to ground surface at the well, where negative values represent belowground water levels and positive values indicate inundation. We also calculated the average hydroperiod of each site by counting the number of days that the mean daily water level was above the soil surface at the well each year, and averaging across years.

2.4.2   Elevation distributions

Our first line of inquiry was to evaluate the general spatial distribution of elevation at each site. We first calculated site-level omni-directional and directional (0°, 45°, 90°, 135°) semivariograms using the *gstat* package in R (Pebesma 2004 and Gräler, 2016). We calculated directional variograms to test for effects of anisotropy (directional dependence) of elevation. Semivariogram analysis is regularly used in spatial ecology to determine spatial correlation between measurements (Ettema and Wardle, 2002). The sill, which is the horizontal asymptote of the semivariogram, is approximately the total variance in parameter measurements. The nugget is the semivariogram y-intercept, and it represents the parameter variance due to sampling error or the inability of sampling resolution to capture parameter variance at small scales. The larger the difference between the sill and the nugget (the "partial sill"), the more spatially predictable the parameter. If the semivariogram is entirely represented by the nugget (i.e., slope = 0), the parameter is randomly spatially distributed. The semivariogram range is the distance where the semivariogram reaches its sill, and it represents the spatial extent (patch size) of heterogeneity, beyond which data are randomly distributed. When spatial

dependence is present, semivariance will be low at short distances, increase for intermediate distances, and reach its

310 sill when data are separated by large distances. We used detrended elevation models for this analysis to assess more directly the importance of microtopography on elevation variation as opposed to having it obscured by site-level elevation gradients. From these semivariograms we calculated the best-fit semivariogram model among exponential, Matérn, or Matérn with Stein parameterization model forms (Minasny and McBratney, 2005). We also extracted semivariogram nuggets, ranges, sills, and partial sills.

Our second line of inquiry was to evaluate the degree of elevation bimodality in these systems, which is indicative of

315 a positive feedback between hummock growth and hummock height (Eppinga et al., 2008). Based on the classification into hummock or hollow from our delineation algorithm, we plotted site-level detrended elevation distributions for hummocks and hollows and determined a best-fit Gaussian mixture model with Bayesian Information Criteria (BIC) using the *mclust* package (Scrucca et al., 2016) in R (R Core Team, 2018), which uses an expectation-maximization algorithm. Mixture models were allowed to have either equal or unequal variance, and were constrained to a

320 comparison of bimodal versus a unimodal mixture distribution.

2.4.3 Subsurface topographic control on microtopography

We assessed the importance of mineral layer microtopography on soil surface microtopography by comparing the depth-to-mineral-layer measurements with the soil surface elevation TLS measurements. We first calculated the elevation of the mineral layer relative to each site-level datum by subtracting the depth-to-mineral-layer measurement

325 from its co-located soil elevation measurement estimated from the TLS campaign. We then plotted the depth-to-mineral-layer measurement (hereafter referred to as "organic soil thickness") as a function of this mineral layer elevation, noting which points were on hummocks or hollows as determined from the TLS delineation algorithm. We fit linear models to these points and compared the regression slopes to the expected slopes from: 1) a scenario where surface microtopography is simply a reflection of subsurface microtopography (slope = 0, or constant organic soil

330 thickness), and 2) a scenario of flat soil surface where organic soil thickness negatively corresponds to varying mineral layer elevation (slope = -1, or varying soil thickness). The first scenario would indicate that surface microtopography mimics subsurface microtopography, whereas the second would indicate organic matter/surface soil accumulation and smoothing over a varying subsurface topography. Observations above the -1:1 line would indicate surface processes that increase elevation above expectations for a flat surface.

2.4.4 Hydrologic controls on hummock height

To test our hypothesis that hydrology is a broad, site-level control on hummock height, we first regressed site mean hummock height against site mean daily water level. We also conducted a within-site regression of individual hummock heights against their local mean daily water level. To do so, we first calculated a local relative mean water level for each delineated hummock location by subtracting the elevation minimum of the hummock (i.e., the elevation at the base of the hummock) from the site-level mean water level elevation. This calculation assumes that the water level is flat across the site, which is likely valid for the high permeability organic soils at each site, low slopes (<1%), and relatively small areas that we assessed. This within-site regression allowed us to understand more local-scale controls on hummock height.

2.4.5 Hummock spatial distributions

To test whether there was regular spatial patterning of hummocks at each site, we compared the observed distribution of hummocks against a theoretical distribution of hummocks subject to complete spatial randomness (CSR) with the R package *spatstat* (Baddeley et al., 2015). We first extracted the centroids and areas of the hummocks using TopoSeg (Stovall et al., 2019) and created a marked point pattern of the data. Using this point pattern, we conducted a nearest-neighbor analysis (Diggle, 2002), which evaluates the degree of dispersion in a spatial point process (i.e., how far apart on average hummocks are from each other). If hummocks are on average further apart (using the mean nearest neighbor distance, μ_{NN}) compared to what would be expected under CSR (μ_{exp}), the hummocks are said to be overdispersed and subject to regular spacing; if hummocks are closer together than what CSR predicts, they are said to be underdispersed and subject to clustering. We compared the ratio of μ_{NN} and μ_{exp}, where values greater than 1 indicate overdispersion and values below 1 indicate clustering, and calculated a z-score (z_{ANN}) and subsequent p-value to evaluate the significance of overdispersion or clustering (Diggle, 2002, Watts et al., 2014). Z-scores were computed from the difference between μ_{NN} and μ_{exp} scaled by the standard error. We also evaluated the probability distribution of observed nearest neighbor distances to visualize further the dispersion of wetlands in the landscape.

2.4.6 Hummock size distributions

To test the prediction that hummock sizes are constrained by patch-scale negative feedbacks, we plotted site-level rank-frequency curves (inverse cumulative distribution functions) for hummock perimeter, area, and volume. These curves trace the cumulative probability of a hummock dimension (perimeter, area, or volume) being greater than or

equal to a certain value ($P[X{\geq}x]$). We then compared best-fit power ($P[X{\geq}x] = \alpha X^{\beta}$), log-normal ($P[X{\geq}x] = \beta\ln(X) + \beta_0$), and exponential ($P[X{\geq}x] = \alpha e^{\beta X}$) distributions for these curves using AIC values. Power-scaling of these curves occurs where negative feedbacks to hummock size are controlled at the landscape-scale (i.e., hummocks have approximately equal probability to be found at all size classes). Truncated scaling of these curves, as in the case of exponential or lognormal distributions, occurs when negative feedbacks to hummock size are controlled at the patch-scale (Scanlon et al., 2007, Watts et al., 2014).

3 Results

3.1 Hydrology

Hydrology varied across sites, but largely corresponded to hydrogeomorphic categories (Table 2). Depressions sites were the wettest sites (mean daily water level = -0.01 m), followed by transition sites (-0.04 m), and lowland sites (-0.32 m). Lowland sites also exhibited significantly more water level variability than transition or depression sites, whose water levels were consistently within 0.4 m of the soil surface. Although lowland sites exhibited greater water level drawdown during the growing season, they were able to rapidly rise after rain events.

3.2 Elevation distributions

Semivariograms demonstrated much more pronounced elevation variability at depression and transition sites than at lowland sites (Figure 4). In general, lowland sites reached overall site elevation variance (sills, horizontal dashed lines) within 5 meters, but best-fit ranges (dotted vertical lines in Figure 4) were less than 1 m. In contrast, best-fit semivariogram ranges for depression and transition sites were several times greater. Therefore, depression and transitions sites have much larger ranges of spatial autocorrelation for elevation than lowland sites. Semivariograms were all best fit with Matérn models with Stein parameterizations, and nugget effects were extremely small in all cases (average <0.001), which we attribute to the very high precision of the TLS method. As such, partial sills were quite large (i.e., the difference between the sill and nugget), indicating that very little elevation variation is at scales less than our surface model resolution (1 cm); the remaining variation is found over site-level ranges of autocorrelation. We did not observe major differences in directional semivariograms compared to the omnidirectional semivariogram, implying isotropic variability in elevation, and do not present them here.

We observed bimodal elevation distributions at every site, with hummocks clearly belonging to a distinct elevation class separate from hollows (Figure 5). Bimodal mixture models of two normal distributions were always better fit to

the data than unimodal models based on BIC values. Differences in mean elevations between these two classes ranged

390   from 12 cm at the lowland sites to 20 cm at depression sites, and hummock elevations were more variable than hollow

elevations across sites. Across sites, 27±10% of all elevations did not fall into either a hummock or a hollow category,

with lowland sites having considerably more elevations not in these binary categories (36–44%) compared to

depression (22–27%) or transition sites (16–22%). However, we emphasize that even when considering the entire site

elevation distribution (i.e., including elevations that did not fall into a hummock or hollow category), bimodal fits

395   were still better than unimodal fits, but to a lesser extent for lowland sites (Figure S3). Delineated hummocks varied

in number and size across and within sites. We observed the greatest number of hummocks in the depression and

transition sites, with approximately an order of magnitude less hummocks found in lowland sites (Figure 5).

3.3   Subsurface topographic control on microtopography

Across sites, organic soil thickness varied and was greatest at the lowest mineral layer elevations, indicating that

400   surface microtopography is not simply a reflection of subsurface mineral layer topography with constant overlying

organic thickness (as illustrated with 0-slope line in Figure 6). In contrast, at most sites, except for D1 and L2, there

was a strong negative linear relationship between soil thickness and mineral layer elevation, with five sites exhibiting

slopes near -1, which we define as the smooth surface model of soil elevation (dashed -1:1 line in Figure 6). If only

hollows (open circles; Figure 6) were used in the regression, then D1 also exhibited a significant (p<0.001) negative

405   slope in this relationship (-0.4, $R^2 = 0.52$). A majority of depth to mineral layer measurements at D3 were below

detection limit with our 1.2 m steel rod, and all but one measurement at T1 were below detection limit. At sites D2

and L2, there was indication that some hollows were actually better represented by the subsurface reflection model

(i.e., slope = 0). However, at all sites, though to a lesser extent at lowland sites (e.g., L1 and L3), hummocks (closed

circles; Figure 6) tend to plot above hollows and above the -1:1 line, indicating that their elevation is greater than

410   would be expected for a smooth surface model.

3.4   Hydrologic control on hummock height

We observed a significant (p<0.001) positive linear relationship between site level mean hummock height and site

level mean daily water level (Figure 7, top panel). Because lowland sites were clearly influential points on this linear

relationship, we also conducted this regression excluding the lowland sites and still found a significant (p = 0.007)

415   positive linear trend between these variables with reasonable predictive power (R^2=0.8) — wetter sites have on average

have taller hummocks than drier sites. We found very little variability in average hummock heights across sites when relative to site-level mean water level elevation (mean normalized hummock height = 0.31±0.06 m), indicating that hummocks were generally about 30 cm higher than the site mean water level.

Within sites, we also observed clear positive relationships between individual hummock heights and their local mean daily water level (Figure 7, bottom panel). At all but two of the sites (D4 and L1), individual hummock heights within a site were significantly ($p<0.01$) taller at wetter locations than drier locations. Slopes for these individual hummock regressions varied among sites, ranging from 0.4–1.1 (mean±sd = 0.7±0.2), and local hummock mean water level was able to explain 12–56% (mean±sd = 0.36±0.14) of variability in hummock height within a site.

3.5   Hummock spatial distributions

All sites characterized as depressions or transitions exhibited significant ($p <0.001$) overdispersion of hummocks compared to what would be predicted under complete spatial randomness (Figure 8). For these sites, the nearest neighbor ratios ($\mu_{NN}:\mu_{exp}$) indicated that hummocks are 25–30% further apart than would be expected with complete spatial randomness, with spacing ca. 1.5 meters, as evidenced by the narrow distributions in nearest neighbor histograms (Figure 8). In contrast, all lowland sites, while having hummock nearest neighbor distances 2–3 times as far apart as depression of transition sites, were not significantly different than what would be predicted under complete spatial randomness ($p = 0.129, 0.125, 0.04$ for sites L1, L2, and L3, respectively).

3.6   Hummock size distributions

Hummock dimensions (perimeter, area, and volume) were strongly lognormally distributed across sites (Figure 9), though exponential models were typically only slightly worse fits. For each hummock dimension, site fits were similar within site hydrogeomorphic categories, but drier lowland site distributions were clearly different from wetter depression and transition site distributions, which were more similar (Figure 9). Lowland sites had significantly lower ($p < 0.05$) coefficients for hummock property model fits than depression or transition sites, with slopes approximately 20% more negative on average, indicating more rapid truncation of size distributions. Across sites, average hummock perimeter was 4.2±0.8 m, average hummock area was 1.7±0.5 m^2, and average hummock volume was 0.17±0.06 m^3. Hummock areas were typically less than 1 m^2 in size at all sites (Figure 9). Similar to hummock spatial density, hummock area per site (ratio of hummock area to site area) was lower at drier lowland sites (2–5%) compared to wetter depression and transition sites (12–22%) (Figure 5).

4   Discussion

We tested our hypothesis that microtopography in black ash wetlands self-organizes in response to hydrologic drivers (Figure 1) using an array of commonly used diagnostic tests from landscape ecology, including analyses of multimodal elevation distributions, spatial patterning, and patch size distributions. We further analyzed the influence of hydrology on these diagnostic measures and tested a potential null hypothesis that surface microtopography was simply a reflection of subsurface microtopography. Diagnostic test results of elevation bimodality, hummock spatial overdispersion, and truncated hummock areas along with clear hydrologic influence on microtopographic structure provide strong support for our hypothesis.

4.1   Controls on microtopographic structure

Bimodal soil elevation distributions at all sites suggest that the microsite separation into hummocks and hollows is a common attribute of black ash wetlands. Soil elevation bimodality was most evident at the wetter depression and transition sites, where hummocks were more numerous and occupied a higher fraction of overall site area (15–20%). Sharp boundaries between hummocks and hollows were not always observed in soil elevation probability densities (Figure 5), which may be indicative of weak positive feedbacks between primary productivity and elevation (Rietkerk et al., 2004; Figure 1). On the other hand, modeling predictions indicate that if evapoconcentration feedbacks (i.e., that hummocks harvest nutrients from hollows through hydraulic gradients driven by hummock-hollow ET differences) are strong, boundaries between hummocks and hollows will be less sharp (Eppinga et al., 2009), possibly implicating hummock evapoconcentration as an additional feedback to hummock maintenance (Figure 1). Greater levels of soil chloride in hummocks relative to hollows in these systems may be an additional layer of evidence for this mechanism (Diamond et al., 2019).

We also observed clear evidence of decoupling between surface microtopography and mineral layer microtopography at all of our sites. Hollows were best represented by a smooth surface model, with a relatively constant surface elevation despite variable underlying mineral soil elevation. Importantly, we also observed that regardless of underlying mineral layer, hummocks had greater soil thickness than hollows (Figure 6). That is, irrespective of mineral layer microtopography, hummocks are maintained at local elevations that are higher than would be predicted for a smooth soil surface. Moreover, drier lowland (L) sites had less clear patterns in this regard than the wetter depression (D) or transition (T) sites, supporting our hypothesis for hydrology driven hummock development. We also note that some measurement locations had deeper organic soils than we could measure with our rod (particularly at our wettest

sites) and that this is likely further evidence for our contention that hummocks are self-organized mounds on a smooth surface of organic soil, rather than an argument against it. Smoothing of soil surfaces relative to variability in underlying mineral layers or bedrock is observed in other wetland systems where soil creation is dominated by organic matter accumulation (e.g., the Everglades, Watts et al., 2014). This implies that deviations from this smooth organic soil surfaces are related to other surface-level processes, such as spatial variation in organic matter accumulation resulting from hypothesized elevation-productivity feedbacks.

Hummock heights relative to mean site-level water level were approximately 30 cm, aligning with field observations of relatively constant hummock height within sites. Generally consistent hummock height across sites in conjunction with clear bimodality in soil elevations supports the contention that hummocks and hollows are discrete, self-organized ecosystem states (*sensu* Watts et al., 2010). However, variability in site-level hummock heights–especially at depression and transition sites–may partially be attributable to hummocks in non-equilibrium states. From our feedback model (Figure 1), it seems reasonable that within a site, some hummocks may be in growing states (e.g., increasing in height over time via the elevation-productivity positive feedback) and some may be in shrinking states if hydrologic conditions have recently become drier (e.g., decreasing in height via the elevation-respiration negative feedback), the combination of which may result in a distribution of hummock heights centered around an equilibrium hummock height. Future efforts could leverage time-series observations of hummock properties (e.g., area, height and volume), but we note the likely decadal time-scales required to detect hummock growth or shrinkage (Benscoter et al., 2005; Stribling et al., 2007).

Local hydrology exhibited clear control on hummock height, providing evidence for our hypothesis that hummocks are a biogeomorphic response to hydrologic stress in wetlands. We found support for this contention at both the site level and at the hummock level. The tallest hummocks were consistently located in the wettest sites and in the wettest zones within sites. At the site-scale, 85% of the variance in average hummock height could be explained by mean water level alone. Within sites, local mean water level explained on average 35% of the variability in hummock height (Figure 7); prevalence of non-equilibrium hummock states may explain much of the additional variability. The considerable variation in the ability of local water levels to explain hummock height within sites (adjusted R^2 =0.12–0.56), and in the strength of that relationship (linear regression slopes=0.4–1.1) may be attributed to two factors: 1) the across-site flat water level assumption, and 2) lack of long trends for hydrology. The flat water level assumption is likely to be a minor effect in transition sites with deep organic wetland soils (e.g., Nungesser, 2003; Wallis and

Raulings, 2011; Cobb et al., 2017) but could be significant at depression and lowland sites with shallower O horizons.

500   Lack of sufficient data to characterize mean water level may also be an issue at several of our sites, because hummocks likely develop over the course of decades or more, whereas our hydrology data only span three years. To our knowledge, this study represents the first empirical evidence of the positive relationship between hummock height and hydrology in forested wetlands. These results are consistent with previous research on tussocks of northern wet meadows (Peach and Zedler, 2006; Lawrence and Zedler, 2011) and shrub hummocks in brackish wetlands (Wallis

505   and Raulings, 2011). The concordance in hydrologic control in these disparate systems suggests a common mechanism of (organic) soil building and accumulation on hummocks that may result from increased vegetation growth from reduced water stress and/or from transport and accumulation of nutrients (Eppinga et al., 2009; Sullivan et al., 2011; Heffernan et al., 2013, Harris et al., 2019).

4.2   Controls on microtopographic patterning

510   We found clear support for our hypothesis that hummocks are non-randomly distributed in our wettest study sites. Hummocks exhibited spatial overdispersion at all sites, but this overdispersion was only significant at depression and transition sites (Figure 8). Significant spatial overdispersion indicates regular hummock spacing in contrast to clustered distributions or completely random placement. Regular patterning of landscape elements is observed across climates, regions, and ecosystems (Rietkerk and van de Koppel, 2008), and is indicative of negative feedbacks that

515   limit patch expansion (Quinton and Cohen 2019). Our results indicate similar patterning for forested wetland microtopography and, importantly, demonstrate the hydrologic controls on that patterning. Hydrology appears to be a common driver in regular pattern formation in wetlands (Heffernan et al., 2013) and drylands (Scanlon et al., 2007). Thus, water stress—both too much (Eppinga et al., 2009) and too little (Deblauwe et al., 2008; Scanlon et al., 2007)— appears to be an important regulator of patch distribution across the landscape.

520   We observed lognormal hummock size distributions, suggesting that some hummocks may attain very large areas (i.e., over 10 m^2), but the majority of hummocks (~80%) are less than 1 m^2 (Figure 9). This finding aligns with field observations, where most hummocks were associated with a single black ash tree, but some hummocks appeared to have merged to create large patches. Truncated patch size distributions are common in other systems as well, such as the stretched exponential distribution for geographically isolated wetlands (Watts et al., 2014) or the lognormal

525   distribution for desert soil crusts (Bowker et al., 2013). These types of distributions have fewer large patches than would be expected for systems without patch-scale negative feedbacks, and have a central tendency towards a common

patch size. Hence, truncation in hummock size distributions comports with hypothesized patch-scale negative feedbacks (i.e., tree competition for light and/or nutrients) that inhibit expansion. Hummocks at drier lowland sites did not conform to size distributions for wetter depression and transition sites, supporting our hypothesis that the

530   feedbacks that control hummock maintenance and distribution are governed by hydrology and amplified in wetter conditions.. This work adds to recent efforts across climates and systems to use patch size distributions to infer drivers of ecosystem self-organization and response to environmental conditions (Kefi et al., 2007; Maestre and Escudero, 2009; Weerman et al., 2011; Schoelynck et al., 2012; Tamarelli et al., 2017).

Characteristic hummock sizes in association with overdispersion in black ash wetlands suggest that hummocks are

535   laterally limited in size by negative feedbacks on the scale of meters (Manor and Shnerb, 2008). We posit that there are two patch-scale negative feedbacks: 1) overstory competition for nutrients and 2) understory and overstory competition for light. Hummocks associated with black ash trees, which account for more than 85% of measured hummocks, are likely limited in area by the radial growth of the tree's root system. Evapoconcentration feedbacks bring nutrients to the tree roots, limiting the degree to which roots must search for them (Karban, 2008), and therefore

540   limiting root lateral expansion. Indeed, evidence suggests that a majority of fine tree roots occur within hummocks in forested wetland systems (Jones et al., 1996; Jones et al., 2000). Moreover, finite nutrient pools may lead to development of similarly sized nutrient source basins for each hummock, further limiting lateral hummock expansion (Rietkerk et al., 2004; Eppinga et al., 2008). Black ash trees must also compete for light with other ash trees, but leaf area is typically low in these systems (Telander et al., 2015). Low LAI and observed crown shyness (*sensu* Long and

545   Smith, 1992) in black ash wetlands may imply less competition among individuals than would be expected in mixed stands (Franco, 1986). On the other hand, less-than-expected canopy competition for light in the overstory may increase light availability for understory hummock species, and therefore allow subsequent hummock expansion from the understory. Therefore, based on evidence and observations presented here and in Diamond et al. (2019), we suggest that a major difference between microtopography in forested versus non-forested wetland systems will be the size

550   distributions and spacing of hummocks. In other forested systems, hummocks associated with trees will likely be limited in size, exhibiting characteristic sizes and spacing due to local negative feedbacks from the crown competition. In contrast, non-forested wetland hummocks may have a much wider distribution of size classes, where negative feedbacks to hummock expansion may be largely due to local nutrient competition effects (e.g., Eppinga et al. 2008).

4.3 Evidence for patch self-organization

In this work, we used common landscape ecology diagnostics to characterize microtopographic pattern and infer responsible reinforcing processes, including analyses of multimodal distributions of elevation, spatial patterns of hummock patches, and hummock size distributions. Other recent work has used nearly identical diagnostic measurements to infer self-organization of depressional wetland features (~100 m wide) in a karst landscape (Quinton and Cohen 2019), demonstrating the broad utility of the approach and the various spatial scales that pattern may manifest. However, we note that this diagnostic approach alone does not directly implicate hypothesized mechanisms of hummock persistence, and that more measurements are required to support inferences made here. To that end, in complementary work we observed support for the elevation-productivity feedback, where we found hummocks to be loci of higher tree occurrence and biomass, more understory diversity, and greater phosphorus and base cation soil concentrations (Diamond et al., 2019). Further, these associations were most evident in the wettest sites, concordant with the hydrologic controls observed here for hummock height, pattern, and size distributions. Together, these multiple lines of evidence lend strong support for the hydrologically driven self-organization hypothesis of hummock growth and persistence (Figure 1).

4.4 Broader implications

The consequences of wetland microtopography are clear at small scales, but can also scale to influence site- and regional-scale processes. For example, microtopographic expression results in a drastic increase in surface area within wetlands. We conservatively estimate an average of 22% and up to 42% relative increase in surface area due to the presence of hummocks (i.e., additional surface area provided by the sides of hummocks; Table 3). These estimates comport with studies in tussock meadows, where tussocks (ca. 20 cm tall) increased surface area by up to 40% (Peach and Zedler, 2006). Further, increases in the diversity of biogeochemical processes occurring at the individual hummock or hollow scale (Deng et al., 2014) likely aggregate to influence ecosystem functioning at large scales. For example, microtopographic niche expansion allows for local material and solute exchange between hummocks and hollows, creating coupled aerobic-anaerobic conditions with emergent outcomes for denitrification (Frei et al., 2012) and carbon emission (Bubier et al., 1995; Minick et al. 2019ab).

While our results implicate hydrology as a major determinant of microtopographic structure and pattern, microtopography can reciprocally influence system-scale hydraulic properties. Results from our hummock property analysis indicate that hummock volume displacement may be a significant factor in water level dynamics of wetlands.

Specific yield, which governs water level response to hydrologic fluxes, is commonly assumed to be unity when wetlands are inundated. However, inclusion of microtopography may render this assumption invalid, with hummock volumes up to 30% of site volumes (Table 4). These observations are supported in other studies of microtopographic effects of specific yield (Sumner, 2007; McLaughlin and Cohen, 2014; Dettmann and Bechtold, 2016). Therefore, while hydrology exerts clear control on the geometry of hummocks, hummocks may exert reciprocal control on hydrology by amplifying small hydrologic fluxes into large water level variations.

Last, black ash hummocks provide unique microsite conditions that support increased vegetation growth and diversity (Diamond et al. 2019), aligning with observations in other wetland systems (Bledsoe and Shear, 2000; Peach and Zedler, 2006; Økland et al., 2008). Accordingly, recent wetland restoration efforts have begun to use microtopography as a strategy to promote seedling success and long-term project viability (Larkin et al., 2006; Bannister et al., 2013; Lieffers et al., 2017). Specific to our focal system, there are increasing efforts to mitigate potential black ash loss due to the emerald ash borer and possible regime shifts to marsh-like states (Diamond et al., 2018). We posit that hummock presence and persistence may allow for future tree seedlings to survive wetting up periods following this ash loss (Slesak et al., 2014), and for consequent resilience of forested ecosystem states.

Overall, this study adds to the growing body of evidence that the structure and regular patterning of wetland microtopography is an autogenic response to hydrology. Although the imprint of biota on landscapes may be masked by the signature of larger scale physical processes (Dietrich and Perron, 2006), we show clear evidence here for a microtopographic signature of life.

5   Code and data availability

The authors will provide code and data upon request, and will upload code to Github upon acceptance of the manuscript. The algorithm for delineating hummocks and hollows ("TopoSeg") can be found at: https://github.com/aestovall/TopoSeg.

6   Author contribution

JD and DM created the conceptual framework, questions, and hypotheses. AS and JD developed the TLS procedure and carried out measurements and subsequent analysis/code; JD and RS carried out hydrology measurements. JD

conducted all data analysis and wrote the manuscript. All co-authors contributed significantly to editing the manuscript.

7 Competing interests

610 The authors declare that they have no conflict of interest.

8 Acknowledgments

This project was funded by the Minnesota Environmental and Natural Resources Trust Fund, the USDA Forest Service Northern Research Station, and the Minnesota Forest Resources Council. Additional funding was provided by the Virginia Tech Forest Resources and Environmental Conservation department, the Virginia Tech Institute for Critical

615 Technology and Applied Science, and the Virginia Tech William J. Dann Fellowship. JD is supported by POI FEDER Loire n°2017-EX001784, Water Agency of Loire Catchment AELB, and University of Tours. We gratefully acknowledge the field work and data collection assistance provided by Mitch Slater, Alan Toczydlowksi, and Hannah Friesen. The authors also acknowledge two anonymous reviewers and Dr. Victor Lieffers, whose comments and suggestions improved this manuscript.

620 **9 References**

Amundson, R., Richter, D. D., Humphreys, G. S., Jobbágy, E. G., and Gaillardet, J.: Coupling between biota and earth materials in the critical zone, Elements, 3(5), 327–332, 2007.

Baddeley A., Rubak, E., and Turner, R.: Spatial Point Patterns: Methodology and Applications with R. London: Chapman and Hall/CRC Press, 2015, URL http://www.crcpress.com/Spatial–Point–Patterns–Methodology–and–

625 Applications–with–R/Baddeley–Rubak–Turner/9781482210200/, 2015.

Bannister, J. R., Coopman, R. E., Donoso, P. J., and Bauhus, J.: The Importance of Microtopography and Nurse Canopy for Successful Restoration Planting of the Slow–Growing Conifer Pilgerodendron uviferum, Forests 4:85–103, 2013.

Barry, W.J., Garlo, A.S. and Wood, C.A.: Duplicating the mound-and-pool microtopography of forested wetlands,

630 Restoration & Management Notes, 14(1), 15–21, 1996.

Benscoter, B.W., Kelman Wieder, R. and Vitt, D.H.: Linking microtopography with post-fire succession in bogs, Journal of Vegetation Science, 16(4), pp.453-460, 2005.

Bertolini, C., Cornelissen, B., Capelle, J., Van De Koppel, J. and Bouma, T.J.: Putting self-organization to the test: labyrinthine patterns as optimal solution for persistence, Oikos, doi: 10.1111/oik.06373, 2019.

635 Belyea, L. R., and Baird, A. J.: Beyond "the limits to peat bog growth", Cross-scale feedback in peatland development. Ecological Monographs, 76(3), 299–322, 2006.

Bledsoe, B. P. and Shear, T. H.: Vegetation along hydrologic and edaphic gradients in a North Carolina coastal plain creek bottom and implications for restoration, Wetlands, 20:126–147, 2000.

Bowker, M. A., Maestre, F. T., and Mau, R. L.: Diversity and patch–size distributions of biological soil crusts regulate
640 dryland ecosystem multifunctionality, Ecosystems, 16(6), 923–933, 2013

Brantley, S. L., Eissenstat, D. M., Marshall, J. A., Godsey, S. E., Balogh-Brunstad, Z., Karwan, D. L., and Chadwick, O.: Reviews and syntheses: on the roles trees play in building and plumbing the critical zone, Biogeosciences (Online), 14(22), 2017.

Bubier, J. L., Moore, T. R., Bellisario, L., Comer, N. T., and Crill, P. M.: Ecological controls on methane emissions
645 from a northern peatland complex in the zone of discontinuous permafrost, Manitoba, Canada, Global Biogeochemical Cycles, 9(4), 455–470, 1995.

Cobb, A. R., Hoyt, A. M., Gandois, L., Eri, J., Dommain, R., Salim, K. A., and Harvey, C. F.: How temporal patterns in rainfall determine the geomorphology and carbon fluxes of tropical peatlands, Proceedings of the National Academy of Sciences, 114(26), E5187–E5196, 2017.

650 Conner, W. H.: Woody plant regeneration in three South Carolina Taxodium/Nyssa stands following Hurricane Hugo, Ecological Engineering 4:227–287, 1995.

Corenblit, D., Baas, A. C., Bornette, G., Darrozes, J., Delmotte, S., Francis, R. A., and Steiger, J.: Feedbacks between geomorphology and biota controlling Earth surface processes and landforms: a review of foundation concepts and current understandings, Earth–Science Reviews, 106(3–4), 307–331, 2011.

655 Courtwright, J. and Findlay, S. E., Effects of microtopography on hydrology, physicochemistry, and vegetation in a tidal swamp of the Hudson River, Wetlands, 31(2), 239–249, 2011.

D'Amato, A., Palik, B., Slesak, R., Edge, G., Matula, C., and Bronson, D.: Evaluating Adaptive Management Options for Black Ash Forests in the Face of Emerald Ash Borer Invasion, Forests, 9(6), 348, 2018.

Deblauwe, V., Barbier, N., Couteron, P., Lejeune, O., and Bogaert, J.: The global biogeography of semi-arid periodic

660   vegetation patterns, Global Ecology and Biogeography, 17(6), 715–723, 2008.

Deng, Y., Cui, X., Hernández, M., and Dumont, M. G.: Microbial Diversity in Hummock and Hollow Soils of Three

Wetlands on the Qinghai–Tibetan Plateau Revealed by 16S rRNA Pyrosequencing, PLOS ONE 9:e103115, 2014.

Dettmann, U., and Bechtold, M.: One-dimensional expression to calculate specific yield for shallow groundwater

systems with microrelief, Hydrological Processes, 30(2), 334–340, 2016.

665   Dietrich, W. E., and Perron, J. T.: The search for a topographic signature of life, Nature, 439(7075), 411, 2006.

Diggle, P.J.: Statistical Analysis of Spatial Point Patterns, 2nd edn. Hodder Education: London; 288, 2002.

Duberstein, J. A., Krauss, K. W., Conner, W. H., Bridges Jr., W. C., and Shelburne, V.B.: Do Hummocks Provide a

Physiological Advantage to Even the Most Flood Tolerant of Tidal Freshwater Trees?, Wetlands 33: 399–408, 2013.

Eppinga, M.B., Rietkerk, M., Borren, W., Lapshina, E.D., Bleuten, W. and Wassen, M.J.: Regular surface patterning

670   of peatlands: confronting theory with field data, Ecosystems, 11(4), 520-536, 2008.

Eppinga, M. B., De Ruiter, P. C., Wassen, M. J., and Rietkerk, M.: Nutrients and hydrology indicate the driving

mechanisms of peatland surface patterning, The American Naturalist, 173(6), 803–818, 2009.

Erdmann, G. G., Crow, T. R., Ralph Jr, M., and Wilson, C. D.: Managing black ash in the Lake States. General

Technical Report NC–115. St. Paul, MN: US Dept. of Agriculture, Forest Service, North Central Forest Experiment

675   Station, 115, 1987.

Ettema, C. H. and Wardle, D. A.: Spatial soil ecology, Trends in ecology and evolution, 17(4), 177–183, 2002.

Foti, R., del Jesus, M., Rinaldo, A., and Rodriguez–Iturbe, I.: Hydroperiod regime controls the organization of plant

species in wetlands, Proceedings of the National Academy of Sciences, 109(48), 19596–19600, 2012.

Franco, M.: The influence of neighbours on the growth of modular organisms with an example from trees,

680   Philosophical Transactions of the Royal Society of London. B, Biological Sciences, 313(1159), 209–225, 1986.

Frei, S., Knorr, K. H., Peiffer, S., and Fleckenstein, J. H.: Surface micro-topography causes hot spots of

biogeochemical activity in wetland systems: A virtual modeling experiment, Journal of Geophysical Research:

Biogeosciences, 117(G4), 2012.

Gabet, E. J., Perron, J. T., and Johnson, D. L.: Biotic origin for Mima mounds supported by numerical modelling,

685   Geomorphology, 206, 58–66, 2014.

Gräler, B., Pebesma, E., and Heuvelink, G.: Spatio–Temporal Interpolation using gstat, The R Journal 8(1), 204–218, 2016.

Harris, L.I., Roulet, N.T. and Moore, T.R..: Mechanisms for the Development of Microform Patterns in Peatlands of the Hudson Bay Lowland, Ecosystems, pp.1-27, 2019.

690 Heffernan, J. B., Watts, D. L., and Cohen, M. J.: Discharge competence and pattern formation in peatlands: a meta–ecosystem model of the Everglades ridge–slough landscape, PloS one, 8(5), e64174, 2013.

Huenneke, L. F., and Sharitz, R. R.: Substrate heterogeneity and regeneration of a swamp tree, Nyssa aquatic, American Journal of Botany, 77(3), 413–419, 1990.

Jackson, R. B., and Caldwell, M. M.: Integrating resource heterogeneity and plant plasticity: modelling nitrate and

695 phosphate uptake in a patchy soil environment, Journal of Ecology, 891–903, 1996.

Jones, R.H., Lockaby, B.G. and Somers, G.L.: Effects of microtopography and disturbance on fine-root dynamics in wetland forests of low-order stream floodplains, American Midland Naturalist, 57–71, 1996.

Jones, R.H., Henson, K.O. and Somers, G.L.: Spatial, seasonal, and annual variation of fine root mass in a forested wetland, Journal of the Torrey Botanical Society, 107–114, 2000.

700 Karban, R.: Plant behaviour and communication. Ecology letters, 11(7), 727–739, 2008.

Kéfi, S., Rietkerk, M., Alados, C. L., Pueyo, Y., Papanastasis, V. P., ElAich, A., and De Ruiter, P. C.: Spatial vegetation patterns and imminent desertification in Mediterranean arid ecosystems, Nature, 449(7159), 213, 2007.

Kéfi, S., Rietkerk, M., Roy, M., Franc, A., De Ruiter, P. C., and Pascual, M.: Robust scaling in ecosystems and the meltdown of patch size distributions before extinction, Ecology letters, 14(1), 29–35, 2011.

705 Koponen, P., Nygren, P., Sabatier, D., Rousteau, A., and Saur, E.: Tree species diversity and forest structure in relation to microtopography in a tropical freshwater swamp forest in French Guiana, Plant Ecology, 173(1), 17–32, 2004.

Kurmis, V., and Kim, J. H.: Black ash stand composition and structure in Carlton County, Minnesota, 1989.

Larkin, D. J., Vivian-Smith, G., and Zedler, J.B.: Topographic heterogeneity theory and ecological restoration. In: Falk, D. A., Palmer, M.A., and Zedler, J.B., (eds), Foundations of restoration ecology. Island Press, Washington, D.C.,

710 USA, 2006.

Larsen, L. G., and Harvey, J. W.: Modeling of hydroecological feedbacks predicts distinct classes of landscape pattern, process, and restoration potential in shallow aquatic ecosystems, Geomorphology, 126(3–4), 279–296, 2011.

Lashermes, B., Foufoula-Georgiou, E., and Dietrich, W. E.: Channel network extraction from high resolution topography using wavelets, Geophysical Research Letters, 34(23), 2007.

715   Lawrence, B. A., and Zedler, J. B.: Formation of tussocks by sedges: effects of hydroperiod and nutrients, Ecological Applications, 21(5), 1745–1759, 2011.

Lieffers, V. J., Caners, R.T., and Ge, H.: Re-establishment of hummock topography promotes tree regeneration on highly disturbed moderate–rich fens, Journal of Environmental Management, 197:258–264, 2017.

Long, J. N., and Smith, F. W.: Volume increment in Pinus contorta var. latifolia: the influence of stand development

720   and crown dynamics, Forest Ecology and Management, 53(1-4), 53–64, 1992.

Maestre, F. T., and Escudero, A.: Is the patch size distribution of vegetation a suitable indicator of desertification processes?, Ecology, 90(7), 1729–1735, 2009.

Manor, A., and Shnerb, N. M.: Facilitation, competition, and vegetation patchiness: from scale free distribution to patterns, Journal of theoretical biology, 253(4), 838–842, 2008.

725   McLaughlin, D. L., and Cohen, M. J.: Ecosystem specific yield for estimating evapotranspiration and :groundwater exchange from diel surface water variation, Hydrological Processes, 28(3), 1495–1506, 2014.

Miao, G., Noormets, A., Domec, J. C., Trettin, C. C., McNulty, S. G., Sun, G., and King, J. S.: The effect of water level fluctuation on soil respiration in a lower coastal plain forested wetland in the southeastern US, Journal of Geophysical Research: Biogeosciences, 118(4), 1748-1762, 2013.

730   Miao, G., Noormets, A., Domec, J.C., Fuentes, M., Trettin, C.C., Sun, G., McNulty, S.G. and King, J.S.: Hydrology and microtopography control carbon dynamics in wetlands: Implications in partitioning ecosystem respiration in a coastal plain forested wetland, Agricultural and forest meteorology, 247, 343-355, 2017.

Minasny, B., and McBratney, A. B.: The Matérn function as a general model for soil variograms, Geoderma, 128(3–4), 192–207, 2005.

735   Minick, K. J., Mitra, B., Li, X., Noormets, A., and King, J.: Water level drawdown alters soil and microbial carbon pool size and isotope composition in coastal freshwater forested wetlands, Frontiers in Forests and Global Change, 2, 7, 2019a.

Minick, K. J., Kelley, A. M., Miao, G., Li, X., Noormets, A., Mitra, B., and King, J. S.: Microtopography Alters Hydrology, Phenol Oxidase Activity and Nutrient Availability in Organic Soils of a Coastal Freshwater Forested

740   Wetland, Wetlands, 39(2), 263-273, 2019b.

Nungesser, M. K.: Modelling microtopography in boreal peatlands: hummocks and hollows, Ecological Modelling, 165(2–3), 175–207, 2003.

Økland, R. H., Rydgren, K., and Økland, T.: Species richness in boreal swamp forests of SE Norway: The role of surface microtopography, Journal of Vegetation Science, 19(1), 67–74, 2008.

745 Othmani, A., Piboule, A., Krebs, M., Stolz, C., Voon, L.L.Y.: Towards automated and operational forest inventories with T–Lidar, in: 11th International Conference on LiDAR Applications for Assessing Forest Ecosystems (SilviLaser 2011), 2011.

Pascual, M., Roy, M., Guichard, F., and Flierl, G.: Cluster size distributions: signatures of self–organization in spatial ecologies, Philosophical Transactions of the Royal Society of London. Series B: Biological Sciences, 357(1421), 657–

750 666, 2002.

Pascual, M., and Guichard, F.: Criticality and disturbance in spatial ecological systems, Trends in ecology and evolution, 20(2), 88–95, 2005.

Pau, G., Fuchs, F., Sklyar, O., Boutros, M., Huber, W.: EBImage—an R package for image processing with applications to cellular phenotypes, Bioinformatics 26, 979–981. https://doi.org/10.1093/bioinformatics/btq046, 2010.

755 Pawlik, Ł., Phillips, J. D., and Šamonil, P.: Roots, rock, and regolith: Biomechanical and biochemical weathering by trees and its impact on hillslopes—A critical literature review, Earth–science reviews, 159, 142–159, 2016.

Peach, M., and Zedler, J. B.: How tussocks structure sedge meadow vegetation. Wetlands, 26(2), 322–335, 2006.

Pebesma, E.J.: Multivariable geostatistics in S: the gstat package, Computers and Geosciences, 30: 683–691, 2004.

Peterson, J. E., and Baldwin, A.H.: Variation in wetland seed banks across a tidal freshwater landscape, American

760 Journal of Botany 91:1251–1259, 2004.

Planchon, O., Esteves, M., Silvera, N., and Lapetite, J. M.: Microrelief induced by tillage: measurement and modelling of surface storage capacity, Catena, 46(2–3), 141–157, 2002.

Pugnaire, F. I., Haase, P., and Puigdefabregas, J.: Facilitation between higher plant species in a semiarid environment, Ecology, 77(5), 1420–1426, 1996.

765 Quintero, C.J. and Cohen, M.J.: Scale-Dependent Patterning of Wetland Depressions in a Low-Relief Karst Landscape, Journal of Geophysical Research: Earth Surface, 124(8), 2101–2117, 2019.

R Core Team: R: A language and environment for statistical computing, R Foundation for Statistical Computing, Vienna, Austria, URL https://www.R–project.org/, 2018.

Reinhardt, L., Jerolmack, D., Cardinale, B. J., Vanacker, V., and Wright, J.: Dynamic interactions of life and its landscape: feedbacks at the interface of geomorphology and ecology, Earth Surface Processes and Landforms, 35(1), 78–101, 2010.

Rietkerk, M., Dekker, S. C., Wassen, M. J., Verkroost, A. W. M., and Bierkens, M. F. P.: A putative mechanism for bog patterning, The American Naturalist, 163(5), 699–708, 2004.

Rietkerk, M., and Van de Koppel, J.: Regular pattern formation in real ecosystems, Trends in ecology and evolution, 23(3), 169–175, 2008.

Roering, J. J., Marshall, J., Booth, A. M., Mort, M., and Jin, Q.: Evidence for biotic controls on topography and soil production, Earth and Planetary Science Letters, 298(1–2), 183–190, 2010.

Roussel, J.R., Auty, D.: lidR: Airborne LiDAR Data Manipulation and Visualization for Forestry Applications, 2018.

Scanlon, T. M., Caylor, K. K., Levin, S. A., and Rodriguez-Iturbe, I.: Positive feedbacks promote power–law clustering of Kalahari vegetation, Nature, 449(7159), 209, 2007.

Scheffer, M., and Carpenter, S. R.: Catastrophic regime shifts in ecosystems: linking theory to observation, Trends in ecology and evolution, 18(12), 648–656, 2003.

Schoelynck, J., De Groote, T., Bal, K., Vandenbruwaene, W., Meire, P., and Temmerman, S.: Self-organised patchiness and scale-dependent bio-geomorphic feedbacks in aquatic river vegetation, Ecography, 35(8), 760–768, 2012.

Schröder, A., Persson, L., and De Roos, A. M.: Direct experimental evidence for alternative stable states: a review, Oikos, 110(1), 3–19, 2005.

Scrucca, L., Fop, M., Murphy, T. B., and Raftery, A. E.: mclust 5: clustering, classification and density estimation using Gaussian finite mixture models, The R Journal 8/1, pp. 205–233, 2016.

Sebestyen, S.D., Dorrance, C., Olson, D.M., Verry, E.S., Kolka, R.K., Elling, A.E., and Kyllander, R.: Chapter 2. Long–term monitoring sites and trends at the Marcell Experimental Forest, In Peatland biogeochemistry and watershed hydrology at the Marcell Experimental Forest. Edited by R.K. Kolka, S.D. Sebestyen, E.S. Verry, and K.N. Brooks. Boca Raton, FL: CRC Press: 15–71, 2011.

Soil Survey Staff, Natural Resources Conservation Service, United States Department of Agriculture. Web Soil Survey. Available online at the following link: https://websoilsurvey.sc.egov.usda.gov/. Accessed February 11, 2019.

Strack, M., Waddington, J. M., Rochefort, L., and Tuittila, E. S.: Response of vegetation and net ecosystem carbon dioxide exchange at different peatland microforms following water level drawdown, Journal of Geophysical Research: Biogeosciences, 111(G2), 2006.

Stovall, A.E., Diamond, J.S., Slesak, R.A., McLaughlin, D.L. and Shugart, H.: Quantifying wetland microtopography with terrestrial laser scanning, Remote Sensing of Environment, 232, 111271, 2019.

Stribling, J. M., Cornwell, J.C., and Glahn, O.A.: Microtopography in tidal marshes: Ecosystem engineering by vegetation?, Estuaries and Coasts 30:1007–1015, 2007.

Sullivan, P. F., Arens, S.J., Chimner, R.A., and Welker, J.M.: Temperature and microtopography interact to control carbon cycling in a high arctic fen, Ecosystems, 11(1), 61–76, 2008.

Sumner, D. M.: Effects of capillarity and microtopography on wetland specific yield, Wetlands, 27(3), 693–701, 2007.

Taramelli, A., Valentini, E., Cornacchia, L., and Bozzeda, F.: A hybrid power law approach for spatial and temporal pattern analysis of salt marsh evolution, Journal of Coastal Research, 77(sp1), 62–72, 2017.

Telander, A. C., Slesak, R. A., D'Amato, A. W., Palik, B. J., Brooks, K. N., and Lenhart, C. F.: Sap flow of black ash in wetland forests of northern Minnesota, USA: Hydrologic implications of tree mortality due to emerald ash borer, Agricultural and forest meteorology, 206, 4–11, 2015.

Turner, M. G.: Landscape ecology: what is the state of the science?, Annu. Rev. Ecol. Evol. Syst., 36, 319–344, 2005.

van de Koppel, J., and Rietkerk, M.: Spatial interactions and resilience in arid ecosystems, The American Naturalist, 163(1), 113–121, 2004.

van De Koppel, J. and Crain, C.M.: Scale–Dependent Inhibition Drives Regular Tussock Spacing in a Freshwater Marsh, The American Naturalist 168:E136–E147, 2006.

von Hardenberg, J., Kletter, A. Y., Yizhaq, H., Nathan, J., and Meron, E.: Periodic versus scale–free patterns in dryland vegetation, Proceedings of the Royal Society B: Biological Sciences, 277(1688), 1771–1776, 2010.

Wallis, E., and Raulings, E.: Relationship between water regime and hummock–building by Melaleuca ericifolia and Phragmites australis in a brackish wetland, Aquatic Botany, 95(3), 182–188, 2011.

Watts, D. L., Cohen, M. J., Heffernan, J. B., and Osborne, T. Z.: Hydrologic modification and the loss of self–organized patterning in the ridge–slough mosaic of the Everglades, Ecosystems, 13(6), 813–827, 2010.

Watts, A. C., Watts, D. L., Cohen, M. J., Heffernan, J. B., McLaughlin, D. L., Martin, J. B., and Kobziar, L. N.: Evidence of biogeomorphic patterning in a low-relief karst landscape, Earth Surface Processes and Landforms, 39(15), 2027–2037, 2014.

825   Weerman, E. J., Van Belzen, J., Rietkerk, M., Temmerman, S., Kéfi, S., Herman, P. M. J., and de Koppel, J. V.: Changes in diatom patch-size distribution and degradation in a spatially self-organized intertidal mudflat ecosystem, Ecology, 93(3), 608–618, 2012.

Western Regional Climate Center [WRCC]: Cooperative Climatological Data Summaries, Retrieved from https://wrcc.dri.edu/cgi–bin/cliMAIN.pl?mn4652, 2019.

830   Wolf, K. L., Ahn, C. and Noe, G.B.: Microtopography enhances nitrogen cycling and removal in created mitigation wetlands, Ecological Engineering 37:1398–1406, 2011.

10 Tables

Table 1 Site information for ten black ash study wetlands

Site	Latitude	Longitude	Elevation (m ASL)	Size (ha)	Average organic horizon depth (cm)
D1	47.67168	-93.68438	447	5.697	28.9 ± 9.1
D2	47.28097	-94.38353	425	6.499	27.7 ± 11.3
D3	47.28380	-94.37992	429	6.062	105.3 ± 32.2
D4	47.28021	-94.48627	442	0.491	60.6 ± 22.1
L1	47.53685	-94.21786	403	2.191	28.8 ± 9.5
L2	47.53444	-94.21320	391	6.845	19.6 ± 7.2
L3	47.52744	-94.20573	394	1.455	24.5 ± 10.1
T1	47.83737	-93.71288	424	15.659	129.4 ± 3.6
T2	47.67887	-93.91441	447	8.618	84 ± 26.2
T3	47.27623	-94.48689	432	1.938	53.6 ± 28.5

835

Table 2 Daily water level summary statistics for black ash study wetlands

Site	Mean (m)	Median (m)	Standard deviation (m)	Mean hydroperiod (d)
D1	0.012	0.088	0.179	105
D2	-0.098	0.042	0.156	96
D3	0.053	0.143	0.196	117
D4	-0.008	0.003	0.151	77
L1	-0.255	-0.046	0.462	67
L2	-0.346	-0.046	0.543	77
L3	-0.370	-0.076	0.502	61
T1	-0.001	0.034	0.125	105
T2	-0.048	0.044	0.202	101
T3	-0.069	0.016	0.217	84

Table 3 Relative area increase by hummocks across sites

Site	Survey area (m²)[†]	Hummock side surface area (m²)[‡]	Relative area increase by hummocks
D1	1045	267	0.26
D2	1041	258	0.25
D3	1093	311	0.28
D4	1164	217	0.19
L1	1234	92	0.07
L2	919	34	0.04
L3	1221	56	0.05
T1	731	304	0.42
T2	994	376	0.38
T3	1198	308	0.26
Average		222±114	0.22±0.13
(Average, no L)		(291±47)	(0.29±0.07)

[†]Survey area is the area scanned by TLS

[‡]Hummock side surface area is calculated from measured volumes and heights using a cone model

840

Table 4 Hummock volume displacement ratios for all sites

Site	Site height[†] (m)	Site volume[‡] (m^3)	Hummock volume (m^3)	Hummock volume displacement ratio
D1	0.17	179	33	0.18
D2	0.15	155	26	0.17
D3	0.21	233	41	0.18
D4	0.17	200	24	0.12
L1	0.15	181	10	0.05
L2	0.26	242	5	0.02
L3	0.21	255	6	0.02
T1	0.18	134	37	0.28
T2	0.16	157	46	0.30
T3	0.17	199	37	0.18
Average			**27±14**	**0.15±0.09**
(Average, no L)			**(35±7)**	**(0.20±0.06)**

[†]Site height is estimated as the mean 80th percentile of hummock heights across the site

[‡]Site volume is estimated as by multiplying site height by site area

 11 Figures
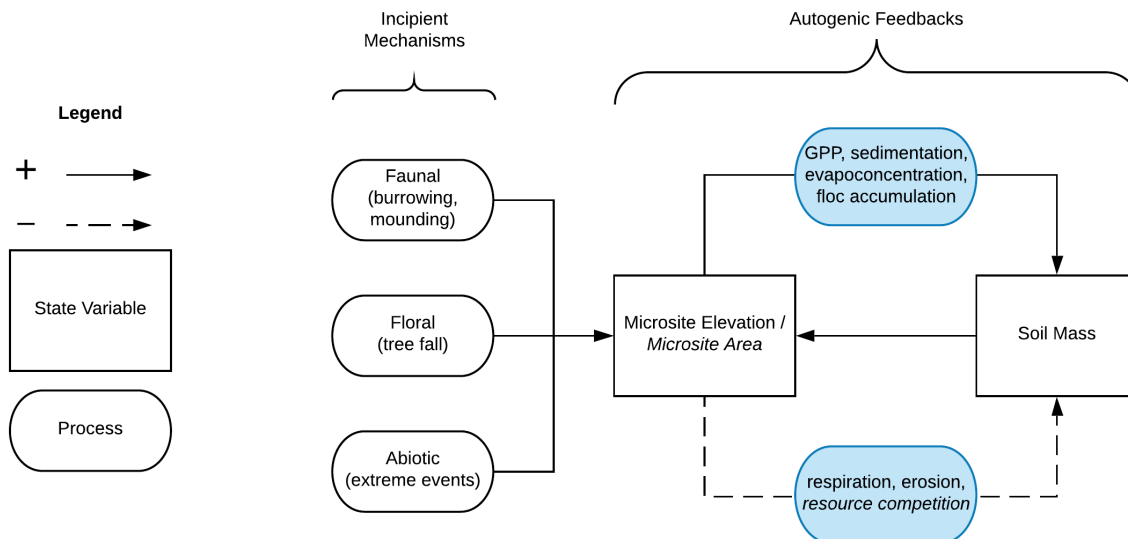
Figure 1. Conceptual model for autogenic hummock maintenance in wetlands. Incipient mechanisms create small-scale variation in soil elevation that is amplified by autogenic feedbacks, which grow and maintain elevated hummock structures. Solid lines indicate positive feedback loops and dashed lines indicate negative feedback loops. Font in italics refer to
850 **feedback processes hypothesized to only affect lateral hummock extent (thus hummock area), whereas non-italic font indicates mechanisms that affect both vertical and lateral hummock extent. Processes in blue indicate that these mechanisms are influenced by hydrology. Soil mass refers to the amount of (organic) soil in a hummock, which can include roots, leaves, and decaying organic matter.**
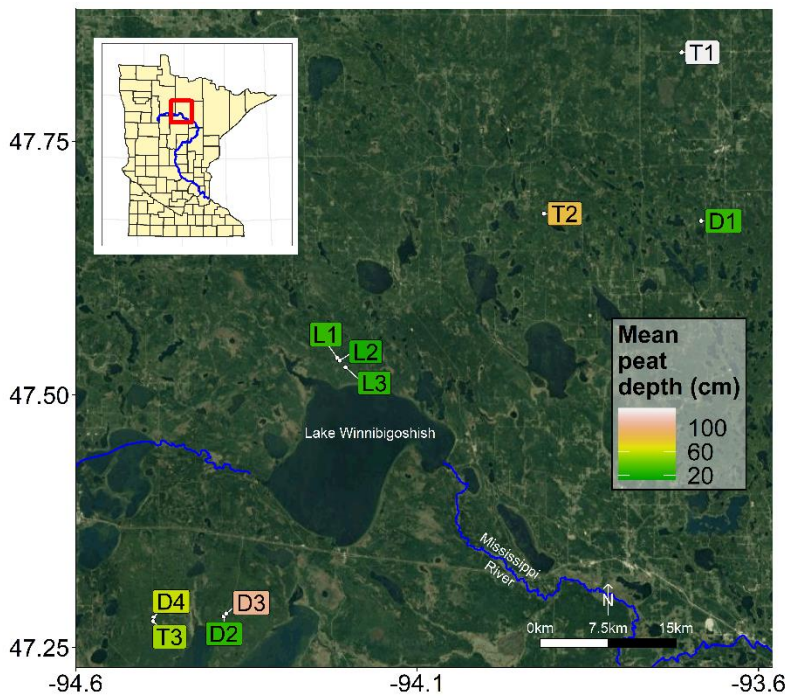
855

Figure 2. Map of black ash wetland sites. Sites are colored by their mean organic horizon depth.
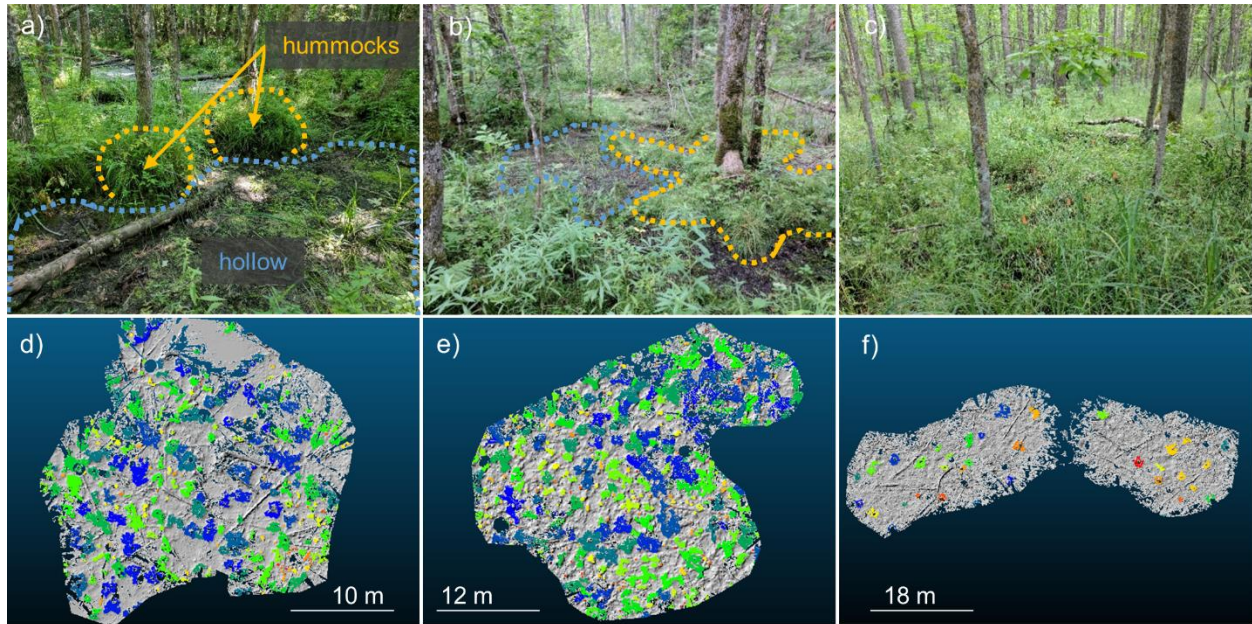
Figure 3. (a–c) Photos of observed black ash wetland microtopography from a site in each hydrogeomorphic category: a) depression site D2, b) transition site T1, and c) lowland site L3. Hummocks are outlined in yellow/orange dashed lines, and hollows are outlined and lightly shaded in blue. Lowland (L1) site hummocks and hollows are difficult to discern in summer time due to heavy understory cover and are additionally less pronounced, so they are not drawn here. In contrast, depression (D2) and transition (T1) site hummocks were typically more visually distinct from hollow surfaces. (d–e) Corresponding automatically delineated hummocks for every site with hill-shaded surface models in the background: d) D2, e) T1, and f) L3. Hummocks are colored in each site by a unique identifier. Although some hummocks have similar colors to their neighbors indicating that they are the same hummock, if they are separated by grey space (hollows), they are unique.
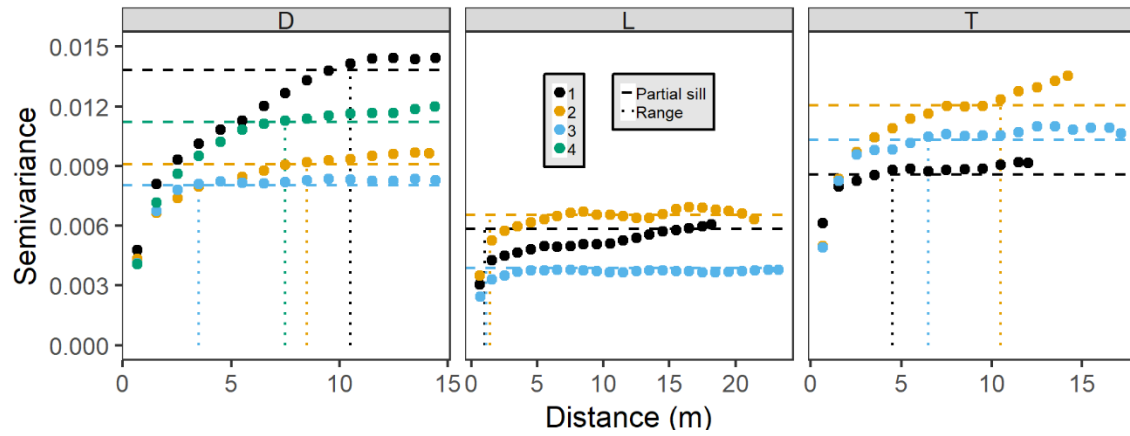
Figure 4. Omni-directional semivariograms for site elevations by hydrogeomorphic category (D = depression, L = lowland, T = transition). Sites are colored according to their number within their hydrogeomorphic category. Dotted vertical lines indicate best-fit ranges and horizontal dashed lines indicate best-fit partial sills (sill – nugget).
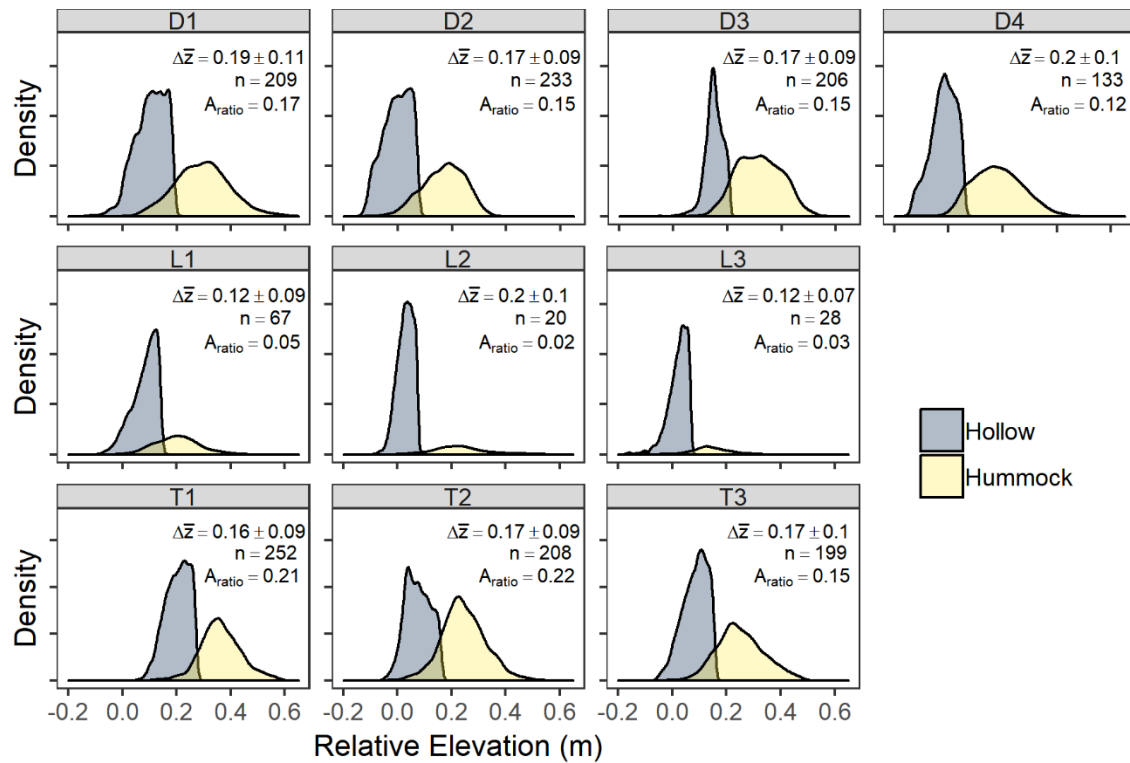
Figure 5. Relative elevation probability densities for each site, colored by hummock and hollow. Text indicates the difference in mean elevation (Δz; m) between hummock and hollow at each site (± standard deviation), the total number of hummocks identified at each site (n), and the ratio of hummock area to total site area (A_{ratio}). Depression sites (D) occupy the top row, followed by lowland sites (L), and transition sites (T). Elevations are relative to the base of the well at each site, which was approximately the lowest elevation at each site.

875
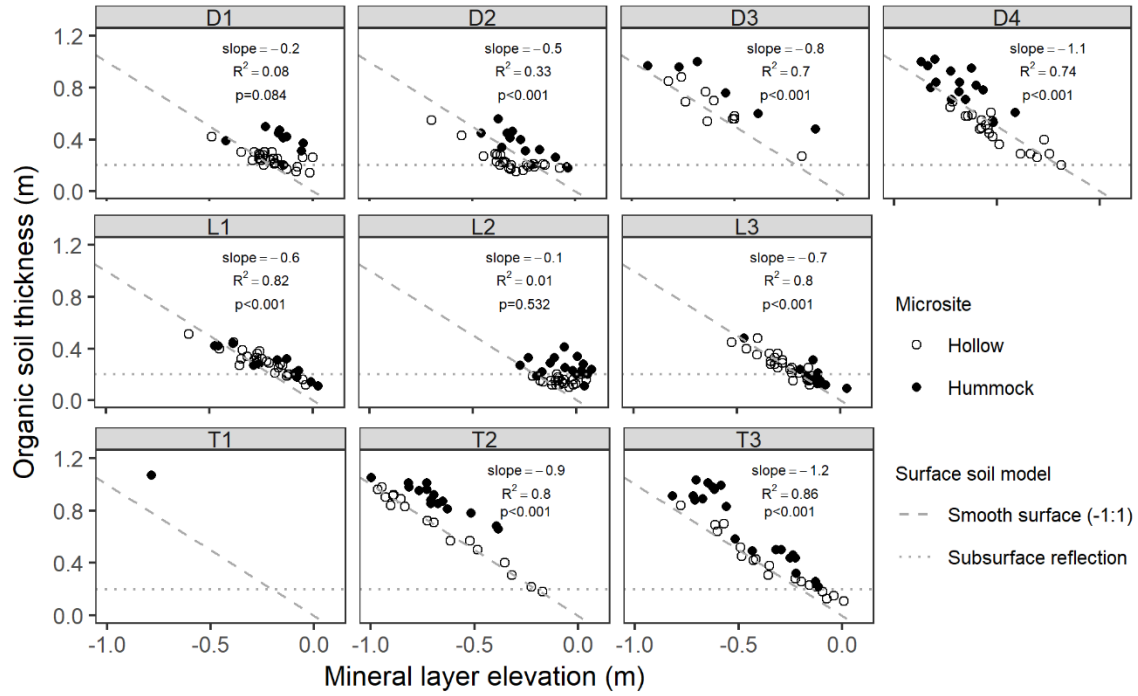
Figure 6. Organic soil thickness (measured as depth to resistance) as a function of mineral layer elevation. Points are filled by their microsite. Dashed -1:1 line indicates a smooth surface soil model and dotted horizontal line indicates a subsurface reflection model. Text values are slopes, R², and p-value of best-fit linear model for aggregated hummock and hollow points.
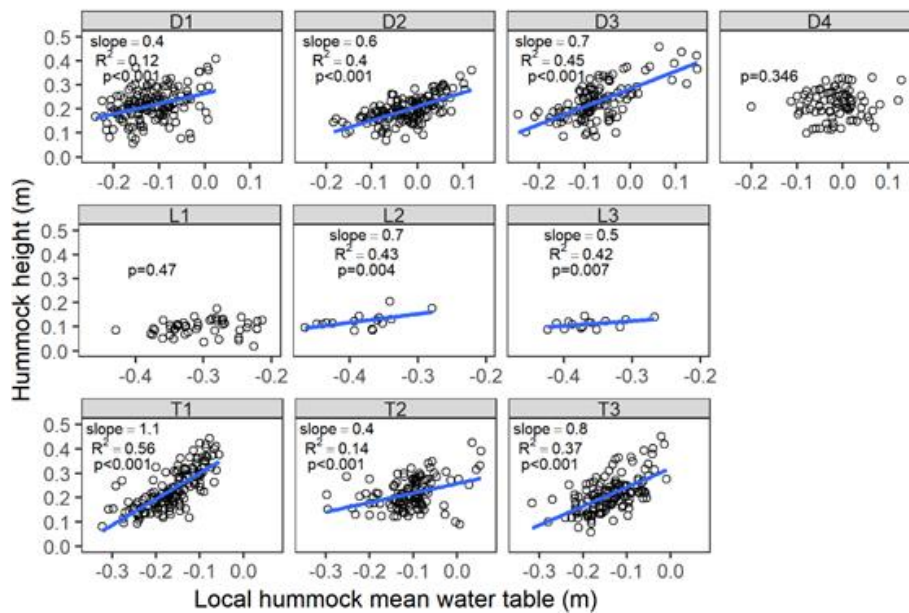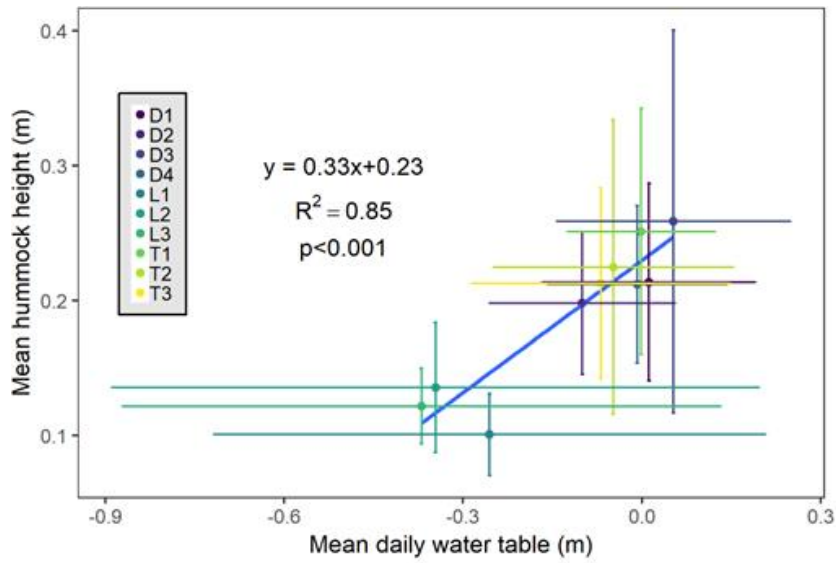
Figure 7. Hummock height as a function of mean water level. (Top) mean site-level hummock height (± sd) versus mean site-level daily water level (± sd), and (Bottom) individual hummock height versus local daily mean water level. Slope, R2, and p-value for best fit linear model (blue line) presented.
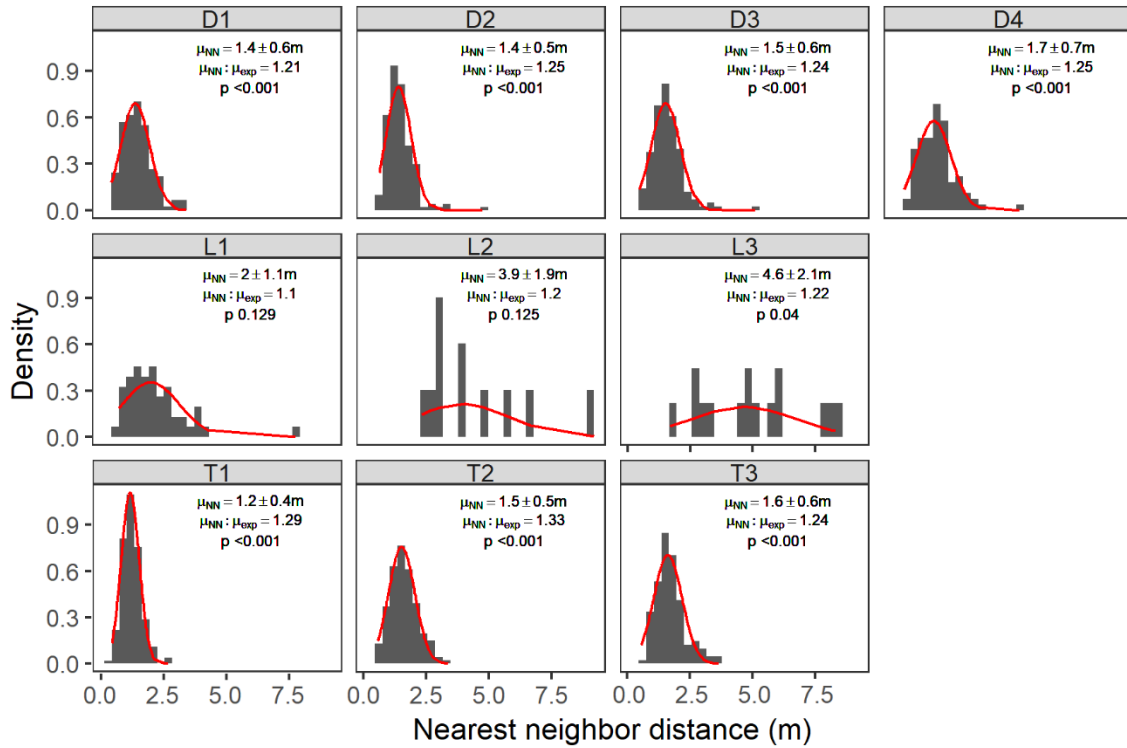
885

Figure 8. Hummock nearest-neighbor distance distributions across sites. Bars are scaled density histograms overlain with best-fit normal distributions (red lines). Text indicates the mean nearest-neighbor distance (μ_{NN} ± standard error); the ratio of the measured mean nearest-neighbor distance and the expected nearest neighbor distance for complete spatial randomness (μ_{exp}); and the p-value for a z-score comparison between μ_{NN} and μ_{exp}. p-values less than 0.001 indicate that
890 **hummocks are significantly overdispersed.**
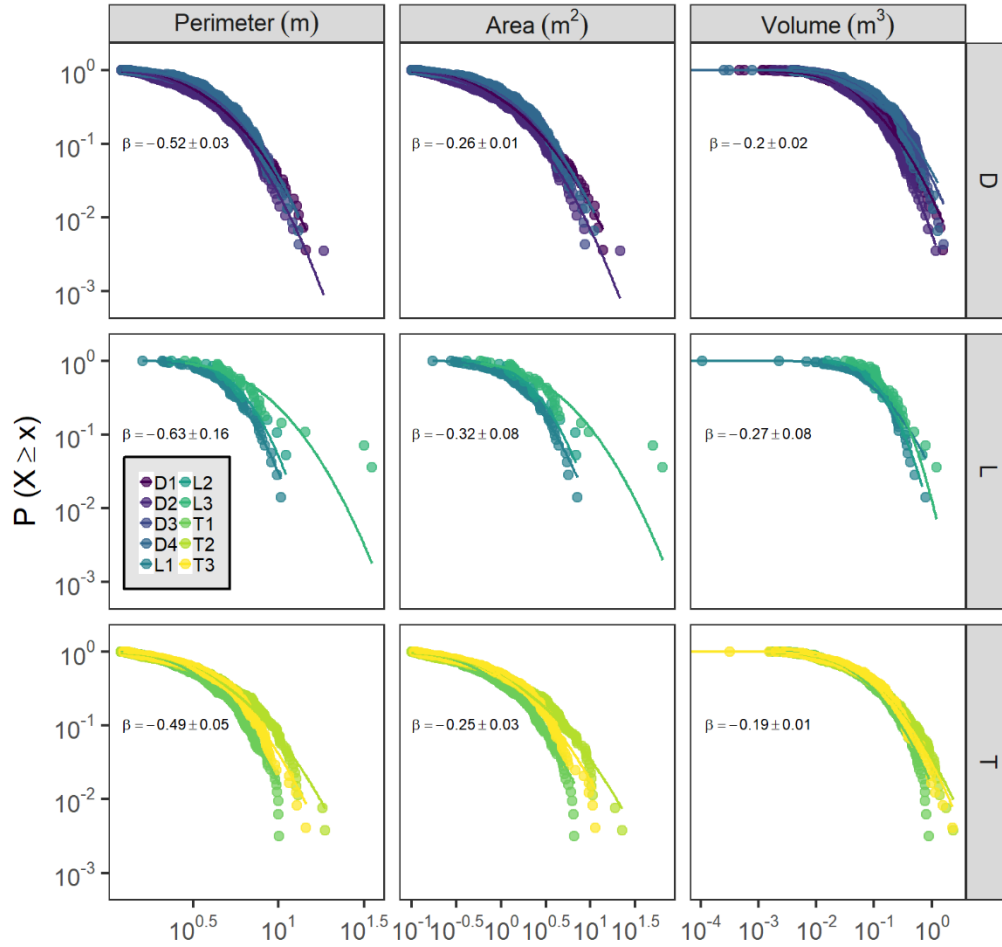
Figure 9. Inverse cumulative distributions of hummock dimensions (perimeter, area, and volume) across sites (points), split by hummock dimension and site type. The y-axis is the probability that a hummock dimension value is greater than or equal to the corresponding value on the x-axis. Best-fit lognormal distributions are shown for each site as lines. All fits were highly significant (p<<0.001). Text indicates mean (±sd) within-group coefficient for a model of the form $P(X \geq x) = \beta * ln(dimension\_value) + \beta 0$.

895